Astron. & Astrophys. 36, 107—111 (1974)

The Non Radial Oscillations of Condensed Polytropes

R. Scuflaire
Institut d'Astrophysique de l'Université de Liège

Received July 3, 1974

Summary. In the adiabatic non radial oscillations of condensed polytropes, the f mode and the first p and g modes show unusual behaviour characterized by the appearance of extra nodes. It is shown that these modes may be interpreted as waves of mixed character, of the internal gravity type in the central regions and of the acoustic type in the external ones.

Key words: non radial oscillations — condensed polytropes

1. Introduction

Polytropic models have largely been used in the study of the non radial adiabatic oscillations of a gaseous sphere (Cowling, 1941; Kopal, 1949; Owen, 1957; Hurley *et al.*, 1966; Robe, 1968). As the central condensation is increased (increasing polytropic index n) the characteristics of the first modes of oscillation are modified (Owen, 1957; Robe, 1968). In this paper it is shown that these modes may be considered as being of the internal gravity wave type in the internal regions of the star and of the acoustic type in the external layers. Dziembowski (1971) was the first to recognize the mixed character of non radial modes in a Cepheid model.

2. Non Radial Oscillations

We have computed the first $l=2$ modes of a sequence of polytropic models whose indices range from 3 to 4.4 with an adiabatic exponent $\Gamma_1 = 5/3$. Thus the domain of condensation ($\varrho_c/\bar{\varrho}$) covered extends from 54.18 to 3.416×10^3. We used Cowling's approximation (Cowling, 1941) which reduces the order of the system of differential equations to 2 (instead of 4).
The radial part of the perturbation obeys Eqs. (1) and (2) (Ledoux and Walraven, 1958).

$$\frac{dv}{dr} = \left[\frac{l(l+1)}{\sigma^2} - \frac{\varrho r^2}{\Gamma_1 P}\right]\frac{P^{2/\Gamma_1}}{\varrho} w, \tag{1}$$

$$\frac{dw}{dr} = \frac{1}{r^2}(\sigma^2 + Ag)\frac{\varrho}{P^{2/\Gamma_1}} v, \tag{2}$$

where

$v = r^2\,\delta r\, P^{1/\Gamma_1}$

$w = \dfrac{P'}{P^{1/\Gamma_1}}$ (P' is the local perturbation of the pressure),

σ is the angular frequency,

l is the degree of the spherical harmonic,

$$A = \frac{d\ln\varrho}{dr} - \frac{1}{\Gamma_1}\frac{d\ln P}{dr}.$$

This approximation gives good results for condensed polytropes as the computations of Robe (1968) have proved.
These equations are very convenient for the analytical discussion but for the numerical computations we use the more appropriate form

$$\frac{dy}{dx} = \frac{l+1}{x}\left[-y + \frac{l}{\omega^2}z\right] + \frac{x}{\Gamma_1}\frac{GM\varrho}{RP}\left(\frac{q}{x^3}y - z\right), \tag{3}$$

$$\frac{dz}{dx} = \frac{1}{x}[\omega^2 y - lz] + RA\left(\frac{q}{x^3}y - z\right), \tag{4}$$

where we have put

$r/R = x$
$m/M = q$
$\delta r/R = x^{l-1}y$
$RP'/GM\varrho = x^l z$
$R^3\sigma^2/GM = \omega^2$.

The regularity condition at the centre imposes

$$\omega^2 y - lz = 0. \tag{5}$$

At the surface, the cancellation of the lagrangian perturbation of the pressure is written

$$\frac{q}{x^3}y - z = 0. \tag{6}$$

In order to determine uniquely the solution we impose the normalizing condition

$$y = 1 \tag{7}$$

at the centre.

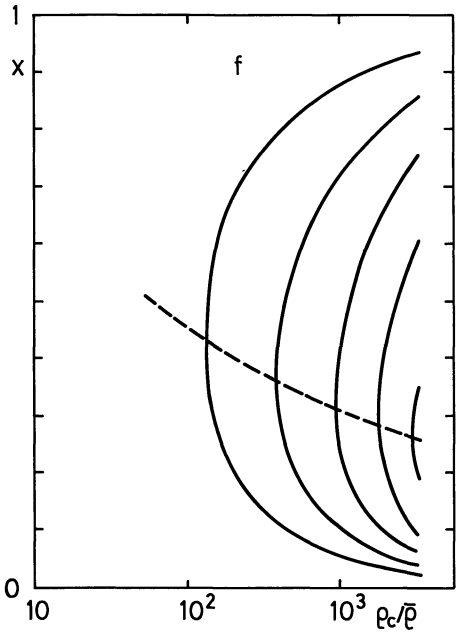

Fig. 1. f mode ($l=2$). Solid lines: positions of the nodes as a function of $\varrho_c/\bar{\varrho}$ in a sequence of polytropic models. Dashed line: locus of appearance of extra nodes

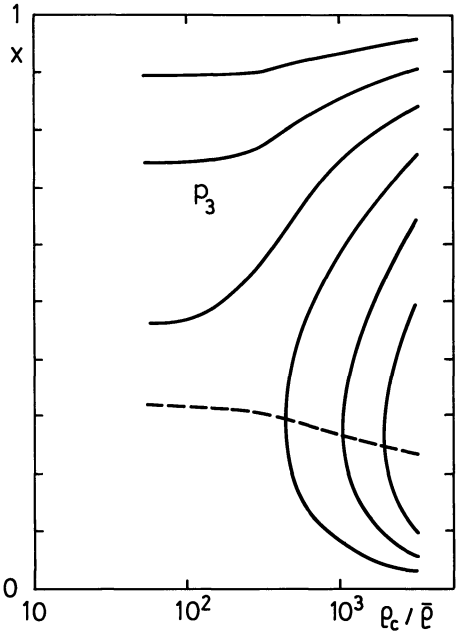

Fig. 2. Same as Fig. 1 but for p_3 mode

With a trial value for ω^2 we integrate Eqs. (3) and (4) with initial conditions (5) and (7) using Runge-Kutta method. Generally this solution does not satisfy Eq. (6) and a new integration is performed with another value of ω^2. This procedure is repeated until Eq. (6) is satisfied, using Newton-Raphson method to improve the value of ω^2.

In the models considered here $A<0$ and all frequencies are real. For the less condensed models the characteristics attributed by Cowling to the different types of modes (f, p and g) do not raise any problem and, for p and g modes, the number of nodes of δr is just equal to the order of the mode. But when the central condensation increases the description becomes more complex (Owen, 1957; Robe, 1968). The f mode acquires two nodes (for $l=2$ this transition takes place for $n=3.4213$, $\varrho_c/\bar{\varrho}=127.52$), then four, etc. The contiguous modes are affected in the same way, they acquire extra nodes by jump of two at a somewhat higher condensation than the f mode. At the same time the general features of these modes are modified. As we shall see later the f and p modes look like g modes in the central regions whereas the f and g modes behave like p modes in the external layers.

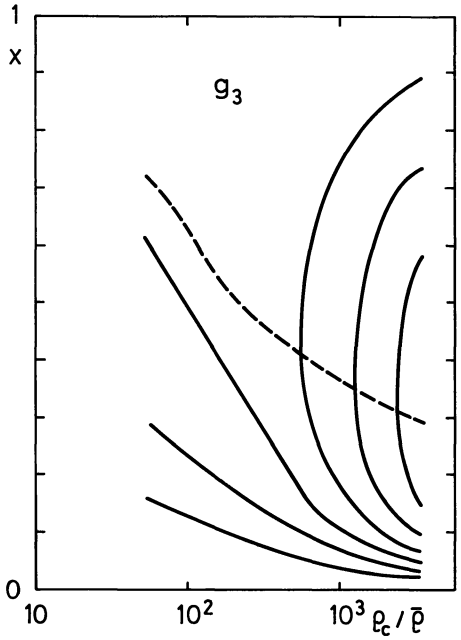

Fig. 3. Same as Fig. 1 but for g_3 mode

Figures 1 to 3 illustrate the appearance of the extra nodes as the condensation increases for $l=2$ modes f, p_3 and g_3. They appear by pair, initially as a double node, and rapidly separate from each other pushing back the existing nodes towards the surface or the center. Let us note that the normal nodes of the p modes (g modes) shift towards the surface (center). The extra nodes appear first at a point where v and dv/dr simultaneously vanishes. At this point one has

$$a=\frac{l(l+1)}{\sigma^2}-\frac{\varrho r^2}{\Gamma_1 P}=0. \tag{8}$$

The locus of these points is represented by a dashed line in Figs. 1 to 3.

3. Space Oscillations of Non Radial Modes

Space oscillation properties of the solutions of Eqs. (1), (2) are related to the signs of the coefficients in the second members of these equations. Space oscillations are allowed only in the regions where these coefficients have opposite signs. This is a consequence of Sturm's

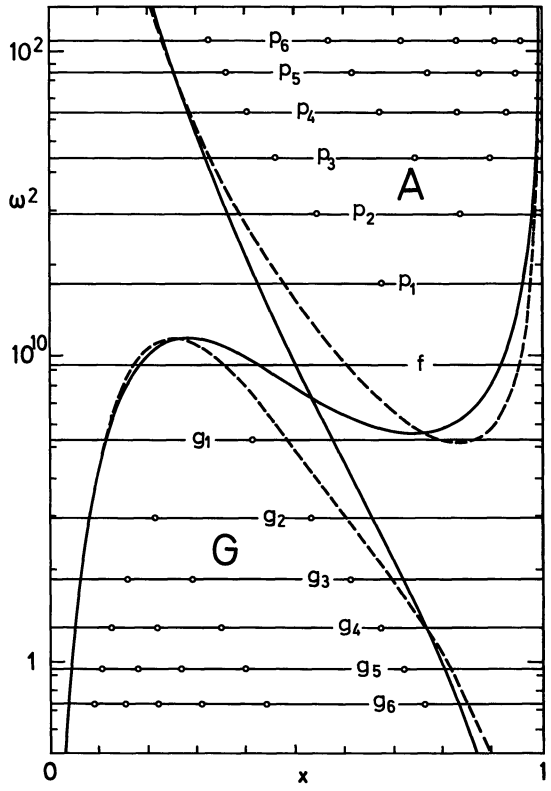

Fig. 4. Polytrope of index 3. The solid lines delimit A and G regions. The horizontal lines give the frequencies of a few modes ($l=2$) and the circles represent the positions of their nodes. The dashed lines represent the cut-off frequencies for plane waves

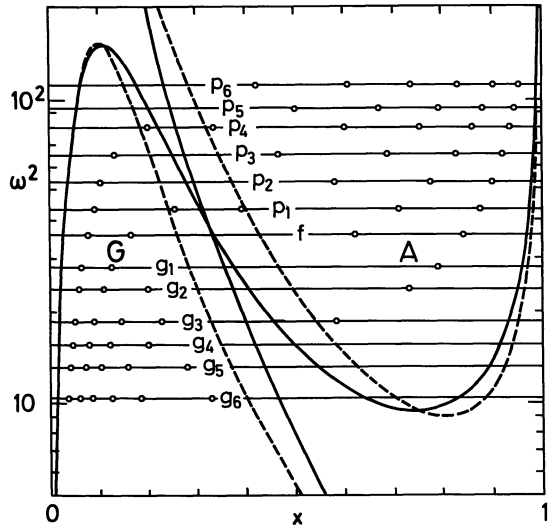

Fig. 5. Same as Fig. 4 but for the polytrope of index 4

oscillation theorem. Though he did not use the same approach, Robe (1968) had already noticed the importance of these coefficients to explain the appearance of extra nodes. The limits of the oscillation regions are defined by Eqs. (8) and (9).

$$b=\sigma^2+Ag=0 \tag{9}$$

or

$$\sigma=N$$

where N is the Väisälä frequency.

In the (x,ω^2) plane, these equations define two curves. We have plotted them (solid lines) for the polytropes $n=3$ (Fig. 4) and $n=4$ (Fig. 5).

We have denoted A and G the regions of this plane corresponding to conditions (position in the star and frequency) allowing spatial oscillations. It is shown in the next section that these regions are characterized by the possibility of existence of progressive acoustic waves and progressive gravity waves respectively. Thus we shall refer to these regions as the acoustic and the gravity regions (or A and G regions). We have also plotted in the same figures the frequencies of the f mode and the first six p and g modes and the positions of their nodes (circles). For the polytrope $n=3$ ($\varrho_c/\bar{\varrho}=54.18$, Fig. 4) all the nodes of the p modes lie in the A region and all the nodes of the g modes lie in the G region as it is expected. But for the more condensed polytrope $n=4$ ($\varrho_c/\bar{\varrho}=622.4$, Fig. 5) the f mode and the first p and g modes have nodes in both regions. We can no longer say that these p modes are purely acoustic modes. They have rather a mixed character: gravity waves in the internal regions and acoustic waves in the external layers. The same is true for the first g modes. This transition from a gravity wave to an acoustic wave is not a new phenomenon. It has been mentioned by Tolstoy (1963) and can also be achieved through a discontinuity. At low condensation the number of nodes is just equal to the order of the mode. When the extra nodes appear this rule is not suppressed, it is only modified: the order of a p mode (g mode) is equal to the number of nodes in the A region (G region) minus the number of nodes in the G region (A region).

The appearance of extra nodes for the more condensed models is explained by the difference of behaviour of the Väisälä frequency throughout the star. For the polytropes of high indices it has two well marked extrema which allow the existence of a large domain of frequency for which an inner part of the star lies in the G region and an outer part of the star lies in the A region.

4. Relations with Plane Waves

The denominations acoustic waves and gravity waves adopted in the preceding section can be justified by a comparison with the theory of plane waves.

In a homogeneous medium any wave can be considered as a superposition of simple waves of the form (monochromatic plane waves)

$$\exp[i(\alpha x+\beta y+\gamma z-\sigma t)]\,.$$

The dispersion equation relates the frequency σ and the three components α, β, γ of the wave number

$$F(\alpha, \beta, \gamma, \sigma) = 0 .$$

In a vertically stratified medium the elementary solutions of the wave equation no longer depend on z by an exponential factor. Nevertheless it is always possible to define the vertical component γ of the wave number (Tolstoy, 1963) so that if $\gamma^2 > 0$ the wave has an oscillatory behaviour in z and if $\gamma^2 < 0$ its behaviour is exponential or hyperbolic. $\gamma^2 > 0$ is also the condition for the existence of progressive waves. If the medium is compressible the dispersion relation may be expressed (Tolstoy, 1963)

$$\gamma^2 = \frac{\sigma^2}{c^2} - \alpha^2 + \frac{\alpha^2}{\sigma^2} N^2 - \frac{1}{4}\left(\frac{d \ln \varrho}{dz}\right)^2 - \frac{1}{2}\frac{d^2 \ln \varrho}{dz^2} \qquad (10)$$

where we have written α^2 for $\alpha^2 + \beta^2$ and c is the speed of sound ($c^2 = \Gamma_1 P/\varrho$). In such a medium the condition for the existence of progressive waves of a given horizontal wave number α reduces to $\sigma > \sigma_1$ (acoustic waves) or $\sigma < \sigma_2$ (gravity waves). The cut-off frequencies are given by

$$\sigma_{1,2}^2 = \frac{c^2}{2}\left\{\alpha^2 + \frac{1}{4}\left(\frac{d \ln \varrho}{dz}\right)^2 + \frac{1}{2}\frac{d^2 \ln \varrho}{dz^2} \pm \sqrt{\Delta}\right\} \qquad (11)$$

with

$$\Delta = \left[\alpha^2 + \frac{1}{4}\left(\frac{d \ln \varrho}{dz}\right)^2 + \frac{1}{2}\frac{d^2 \ln \varrho}{dz^2}\right]^2 - 4\frac{\alpha^2 N^2}{c^2} .$$

These relations are valid for plane geometry. We have however used them for our spherical models with

$$\alpha^2 = \frac{l(l+1)}{r^2}, \qquad (12)$$

$$z = r . \qquad (13)$$

We have plotted (dashed lines) these cut-off frequencies for the polytropes $n = 3$ (Fig. 4) and $n = 4$ (Fig. 5). The domain of acoustic waves lies above the upper dashed curve and the domain of gravity waves lies below the lower curve. The comparison of these domains with the A and G domains is very satisfactory and justifies the denominations adopted in the preceding section.

5. Phase Diagram

The mixed character of the first modes for polytropes of high central condensation is very apparent in the phase diagrams. The variables v and w varies so much from the center to the surface that it is impossible to plot them directly along the axes. However the functions

$$\xi = \pm \lg_{10}\left(1 + \left|\frac{\delta r}{R}\right|\right)$$

$$\zeta = \pm \lg_{10}\left(1 + \left|\frac{RP'}{GM\varrho}\right|\right)$$

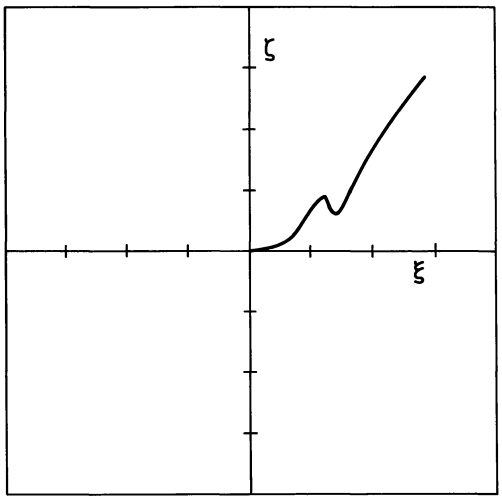

Fig. 6. Phase diagram for the f mode ($l = 2$), polytrope $n = 3$. Each division of the axes represents one unit of ξ or ζ

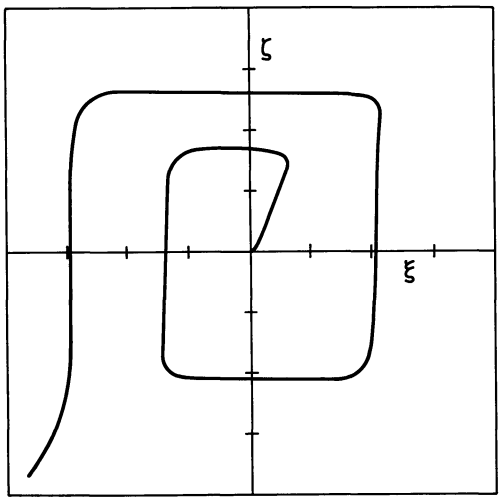

Fig. 7. Same as Fig. 6 but p_3 mode of polytrope $n = 3$

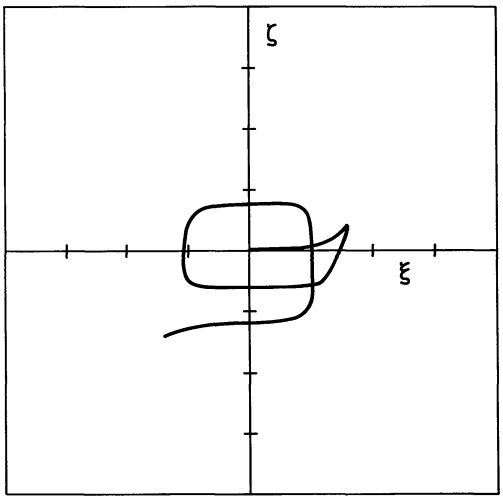

Fig. 8. Same as Fig. 6 but g_3 mode of polytrope $n = 3$

(with the signs chosen according to the signs of the variables) are more appropriate and have been plotted in Fig. 6 to 11. Let us note that the graphs so obtained are approximately linear in $\delta r/R$ and $RP'/GM\varrho$ for the

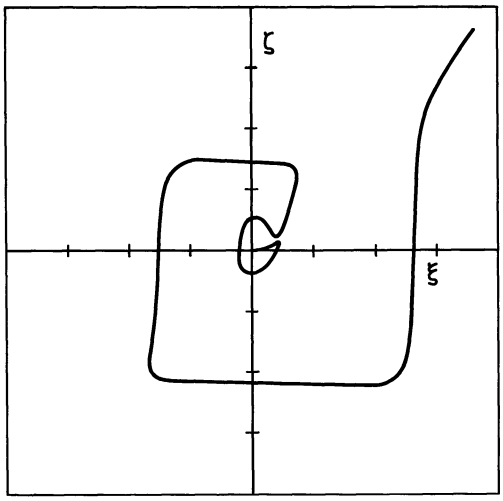

Fig. 9. Same as Fig. 6 but f mode of polytrope $n=4$

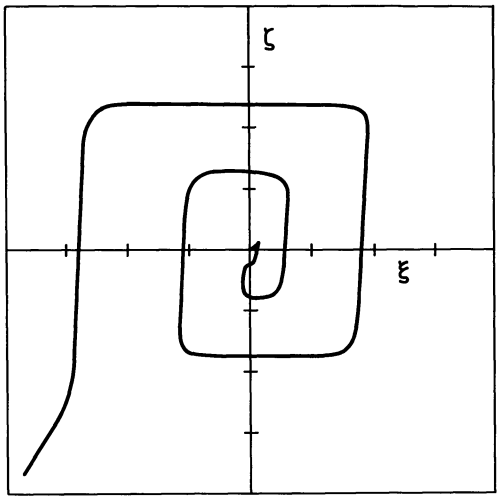

Fig. 10. Same as Fig. 6 but p_3 mode of polytrope $n=4$

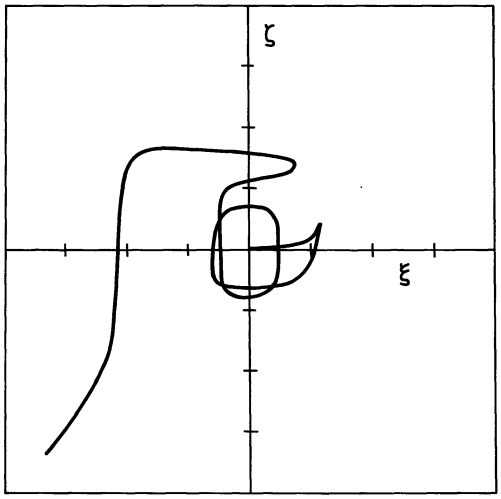

Fig. 11. Same as Fig. 6 but g_3 mode of polytrope $n=4$

small values of the variables and approximately logarithmic for large values of the variables. Eckart (1960) has studied in great details similar phase diagrams and has shown them to be very useful to distinguish the different classes of waves.

For the polytrope of index 3 (Figs. 6, 7 and 8) the number of intersections of the curve with the ordinate axis (the origin excluded) is equal to the order of the mode. p and g modes differ from each other by the sense of rotation of the curve around the origin. This statement is just a generalization of the remark of Cowling (1941) about the first node from the center (node of δr for p modes, node of P' for g modes).
For the more consensed polytrope $n=4$ the phase diagrams (Figs. 9, 10 and 11) indicate clearly the mixed character of the modes. The order of the modes is still equal to the number of intersections with the ordinate axis on the condition to count them positively or negatively according to the sense of rotation.

6. Conclusion

This study emphasizes a new point of view concerning the interpretation of the characteristics of the non radial oscillation modes of highly condensed polytropes.
This brings out the existence in these models of waves of mixed types and gives a simple criterion to identify the order of the mode in presence of extra nodes. The considerations developed here may certainly be extended to physical models. The behaviour of the Väisälä frequency throughout the star is a determining factor for the appearance of mixed modes. This modification in the behaviour of the non radial modes may prove important in the study of vibrational stability. The existence of a great number of nodes, even for the modes of low order, i.e. the existence of a short wavelength, favours a strong radiative damping. This was the case for the Cepheid model studied by Dziembowski (1971). A similar behaviour may be generally expected in very condensed models (very large $\varrho_c/\bar{\varrho}$).

Acknowledgement. It is a pleasure to thank Professor P. Ledoux for helpful discussions and for reading the manuscript.

References

Cowling, T.G. 1941, *Monthly Notices Roy. Astron. Soc.* **101**, 367
Dziembowski, W. 1971, *Acta Astron.* **21**, 239
Eckart, C. 1960, Hydrodynamics of Ocean and Atmospheres, Pergamon Press
Hurley, M., Roberts, P.H., Wright, K. 1966, *Astrophys. J.* **143**, 535
Kopal, Z. 1949, *Astrophys. J.* **109**, 509
Ledoux, P., Walraven, Th. 1958, Variable Stars in Handbuch Physik **51**, 353, Ed. Flügge, Springer, Berlin, Heidelberg, New York
Owen, J.W. 1957, *Monthly Notices Roy. Astron. Soc.* **117**, 384
Robe, H. 1968, *Ann. Astrophys.* **31**, 475
Tolstoy, I. 1963, *Rev. Mod. Phys.* **35**, 207

R. Scuflaire
Institut d'Astrophysique de l'Université de Liège
Avenue de Cointe, 5
B-4200 Ougrée, Belgique